

TOTAL BODY IRRADIATION DOSIMETRY OF A LOW DOSE RATE  $^{60}\text{Co}$   
GAMMA FIELD

MLADEN VRTAR

*Clinic of Oncology and Radiotherapy, University Hospital Centre Rebro, Kišpatičeva 12,  
HR-10000 Zagreb, Croatia*

*E-mail addresses: mlvrtar@sirius.phy.hr, mladen.vrtar@zg.hinet.hr*

**Dedicated to Professor Kseno Ilakovac on the occasion of his 70<sup>th</sup> birthday**

Received 12 September 2001; revised manuscript received 21 January 2002

Accepted 21 January 2002      Online 6 April 2002

An in-vivo dosimetry procedure for direct patient dose reading can help to define deviations of the actually delivered dose from the prescribed one. It is routinely performed by the use of external measurements, i.e. entrance and exit dose readings at certain locations in the body. This article presents a method for the absorbed dose determination of the patient situated in a large  $^{60}\text{Co}$  gamma field, as in total body irradiation (TBI), during in-vivo irradiation and the radiation field analysis at extended distance (in low dose rate conditions) prior to the actual in vivo treatment. The new approach consists of: (1) adjusting the real patient's anatomical data (anterior posterior thickness at a number of points) to the theoretical model of an anthropomorphic phantom of a shape of an elliptical cylinder, and (2) using a n-type silicon field detector with increased sensitivity for the purpose of radiation-field analysis prior to the actual in vivo TBI treatment. Namely, the standard p type field detector, as commercially available for routine radiation field analysis at short distances and high dose rates, was not suitable for radiation field analysis under TBI conditions, because the signal was too weak. Dependence of the calibration factor of the silicon detector, exposed to different dose rates in standard and large field irradiation conditions, was investigated. The detector was found to be suitable for TBI measurements. This was confirmed, among others, in a depth dose curve's behaviour as compared to the results obtained by the standard p-type silicon detector at extended distances.

PACS numbers: 87.53.-j, 87.53.Dq

UDC 539.122

Keywords: in-vivo dosimetry, silicon detector, total body irradiation

## 1. Introduction

There is a continuous effort in standard radiotherapy to reach a high precision in the dose delivery to a target volume. The requirement of the standard deviation of 3.5% has been accepted by many authors [1–4]. That led to the development of quality assurance criteria as the routine tool in clinical practice in the last years. On the other hand, determination of the dose delivered to a body during total body irradiation (TBI) with large  $^{60}\text{Co}$  gamma fields is not easy, because direct measurements are not possible. However, large field irradiation, such as TBI, differs in many aspects from the standard irradiation procedure. In TBI, the target volume is very extended, so we need at least one representative point to which the prescribed dose can be referred. In most cases, and in our case too, this is a mid point of the abdomen at the level of umbilicus. This point is referred as 100%. The dose at other points, which are representatives of certain regions in the body, can be expressed relative to the value at this reference point. So, the requirements on the dose homogeneity undergo the specific conditions and the demand on the above mentioned precision of 3.5% has been lowered in TBI to  $\pm 10\%$ , considering the maximum and minimum dose values in the transverse direction and the direction along the patient's midline [5]. An important reason is the anatomical shape, which defines the various thicknesses of the body regions. The patient is situated in a large irradiation field at a few meters (usually 4 m) from the source, in such a position that the field (about  $1.6\text{ m} \times 1.6\text{ m}$ ) exceeds his (her) size. The usual beam direction is horizontal, and the patient's position is on his side to make the anterior-posterior (AP) (and vice versa PA) irradiation possible. We must point out that the precision of the beam calibration of the radiotherapy machine and the absolute beam calibration in TBI should be much better than the final precision of the dose to the target volume, preferably below  $\pm 5\%$ . Therefore, the beam calibration and the method of radiation field analysis will be considered in this presentation as an important condition in the whole chain of the dose determination procedure.

As pointed out, prior to the actual TBI in vivo treatment, an extensive phantom dosimetry must be performed. There have been several investigations of this type [6–10], but in most of the cited papers, the used models and algorithms, even covering generalized cases, were related to the measurements in cubic phantoms. Concerning the lung dose determination in TBI, there has also been a number of interesting systematic approaches [11–14].

Determination of the absorbed dose under TBI conditions also demands extensive calculations for anthropomorphic phantoms of elliptical-cylinder shape, which can closely approximate the body of a single patient. Once established, the theoretical phantom assigned to the certain patient was included in software and combined with the results of in-vivo dose readings during the treatment. These readings have been done with the "direct patient dose" (DPD) silicon detectors (Scanditronix, Uppsalla), which can distinguish 1 cGy difference in the dose reading, and should be considered as detectors for relative measurements. Semiconductor silicon detectors have been used in clinical practice for many years [15–17]. Namely, the average energy required to form an ion pair in an air-filled ionisation chamber is 33.97 eV,

and to create an electron-hole pair in an n-type Si semiconductor is 3.6 eV. The density of Si is  $2.3 \text{ g/cm}^3$  and that of air is  $0.001293 \text{ g/cm}^3$ . Therefore, one of the most important advantages of the semiconductor detector is the high sensitivity per unit volume, about 18000 times higher than for an ionisation air-filled chamber. That makes possible the use of the DPD detector with a small sensitive volumes and high spatial resolution.

In the use of another type of silicon detector (named radiation field detector (RFD)), needed for radiation field analysis (for depth dose and tissue maximum ratio measurements, when the accuracy should be higher (less than 1 cGy), there are some limitations arising from the overresponse of a silicon detector to photons of energies below 200 keV. For measurements in high-energy photon fields that is not important, because the number of photons with energies below 200 keV is negligible, but in large fields of the photon energies of  $^{60}\text{Co}$  gamma (1.25 MeV), as under TBI conditions, the multiply-Compton-scattered low-energy photons result in overestimation of the depth-dose data. To compensate for this, the sidewalls of RFD have to be covered with a steel or lead cylinder. Also, the presence of radiation damage effect is an obvious drawback and the preirradiation to doses in the kGy region improves the sensitivity variation [18]. It is already known that the statistical noise in the detector reading increases with detectors of smaller volume.

The mentioned field analysis of large cobalt radiation fields must be made for extended distances under TBI conditions, where the dose rate is (for radiotherapy requirements) rather low (1 to 3 cGy/min, depending on the strength of the cobalt source). On the other hand, in these measurements the high spatial resolution is not needed. Therefore, taking all facts into account, it seems rational to enlarge the detector volume in TBI radiation field analysis in order to increase the sensitivity. For this purpose, we used specially designed n-type silicon RFD (prototype, produced in Scanditronix, Uppsalla). The choice of RFD of n-type and DPD detectors for in-vivo dosimetry of p-type is due to the producer. For the monitoring of continuous  $^{60}\text{Co}$  irradiation, the difference is not important [18].

The prescribed dose to the target volume amounted 12.45 Gy in 3 exposures (in 3 days). It means that the low-dose-rate irradiation during one exposure was performed for several hours (usually during the weekend), changing the AP and PA positions (for the homogeneity reasons) of the patient to reach 4.15 Gy per day. The described fractionated irradiation regimen resulted in the evasion in the treatment of 350 patients of the most serious complication, the irradiation-induced pneumonitis, and the lung shielding (applied in the high-dose-rate conditions at linear accelerators) was not needed.

## 2. *Simulation of TBI with phantom and mathematical models*

The basic approach to TBI dosimetry lies in the semiconductor in-vivo dosimetry applied to combined anterior-posterior and posterior-anterior irradiation.

tion method. The absorbed dose  $D_m$  in the patient's mid plane in ten important locations, such as: head (H) neck (N), shoulder (S), mediastinum (M), lung (Lg-without correction), abdomen (A), thigh (T), leg (L), knee (K) and foot (F), can be determined by the use of the entrance (input)  $R_{in}$  and exit (output)  $R_{out}$  dose readings, as measured in the direction of beam's ray passing a considered location. The arithmetic mean of the two readings should be multiplied by the corresponding mid-plane dose factor ( $MDF$ ). In the lung region, an additional correction factor ( $CF$ ) has to be applied. So we have

$$D_m = \frac{R_{in} + R_{out}}{2} MDF \times CF . \quad (1)$$

There are relations between the detector readings  $R_{in}$  and  $R_{out}$ , and the absorbed doses  $D_m$ ,  $D_{in}$  and  $D_{out}$ , defined at the mid-plane point, maximum-ionization point and at exit-surface point, respectively (Fig. 1).  $D_{in}$  and  $D_{out}$  itself can also be expressed by  $D_m$  for the shown geometry. The result is that  $MDF$  could be expressed by tissue maximum ratio ( $TMR$ ) formalism, where  $TMR$  is a ratio of

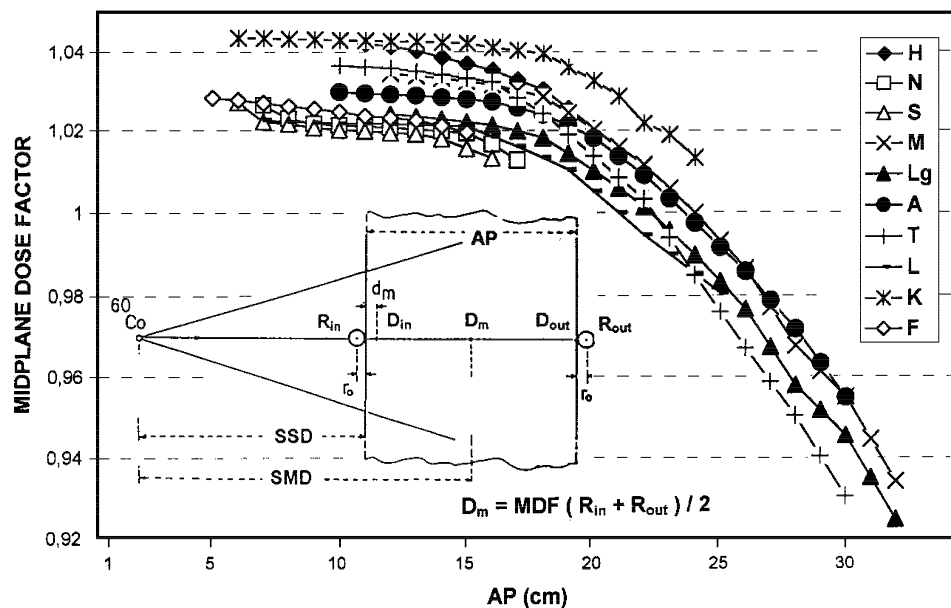


Fig. 1. Geometry of an irradiation in-vivo dosimetric model defining the position of the detector readings  $R_{in}$ ,  $R_{out}$ , absorbed dose points  $D_m$ ,  $D_{in}$ ,  $D_{out}$  and behaviour of mid-plane dose factors ( $MDF$ ) of different locations (head (H), neck (N), shoulder (S), mediastinum (M), lung (Lg-without correction), abdomen (A), thigh (T), leg (L), knee (K) and foot (F)) and their dependence on the AP thickness.

the dose at a given point at depth  $d$  in the phantom to the dose at the same point at the reference depth of maximum dose (0.5 cm for  $^{60}\text{Co}$  gamma irradiation), i.e.  $TMR(d) = D(d)/D_{\text{in}}$ . So we have [21]

$$MDF = \frac{2TMR(AP/2)}{TMR(AP) \left( \frac{SMD}{SMD - AP/2 - r_0} \right)^2 + \left( \frac{SMD}{SMD + AP/2 + r_0} \right)^2}. \quad (2)$$

Here,  $AP$  is the distance between input and output points on phantom surface in the beam's ray direction of a certain location,  $SMD$  is the source to mid-plane distance and  $r_0$  is the radius of the detector, which is fixed on the skin. The most important thing is to determine  $MDF$  for a certain individual case. According to the real patient's data, this factor can be obtained by the use of a theoretical model.

The first experimental and theoretical investigations were performed on a set of 3 types of cubical water-phantoms consisting of more basins with different dimensions, which simulated an anthropomorphic cubical shape of the patient lying on his side. The abdomen thicknesses were 10, 20 and 30 cm, respectively. The middle one with the  $AP$  thickness of abdomen 20 cm, length 150 cm and mass 63 kg, was named as referential cubical phantom (RCP). Subsequently, we measured the dosimetric data on a real anthropomorphic phantom (RAP) filled with water, produced by a sculptor [20], with principal dimensions as in RCP (Fig. 2a). The results were improved because the real shape reflected closer scattering conditions to the patient's dosimetry than the cubic one. The dose to the lung was investigated on experimental polystyrene thorax phantom (combined with wood of different densities, 0.16 and 0.38 g/cm<sup>3</sup>), based on real CT-taken patient's dimensions.

In order to form a theoretical model, a set of mathematically designed circular and elliptical cylinders simulating the real anthropomorphic phantom (RAP) (Fig. 2a) was referred as referential theoretical anthropomorphic phantom (RTAP) (Fig. 2b). The elliptical cylinders had such an arrangement that they represented the RAP (in position, shape, and principal dimensions) as close as possible. A theoretical model, which could reproduce the results of measurements in this experimental water phantom, was based on the following assumptions:

- 1) Absorbed dose was separated into primary and scattered component.
- 2) Sector integration method was adjusted to RTAP under TBI conditions.
- 3) Reduction-of-dose factor, because of the finite phantom thickness, was introduced inside each of 20 phantom parts.
- 4) In the lung region, the equivalent path method was used. (the volumes of experimental right and left lung were 2436 cm<sup>3</sup> and 1698 cm<sup>3</sup>, respectively, and in the theoretical consideration, lungs were represented as parts of elliptical cylinder with volumes of 2410 and 1690 cm<sup>3</sup>, i.e. were less than 1% different than the RAP values).

Taking into consideration all these assumptions, the calculation procedure was performed with a program in Fortran which includes the following main steps.

The total mid plane dose  $D_m(d, r)$ , depending on the depth  $d$  and radius  $r$  of the

local field, at the point T (Fig. 3) consists of the primary and scattered component, i.e.

$$D_m(d, r) = D_p + D_s(d, r). \quad (3)$$

The components are

$$D_p = G_0 f(x_0, y_0) \exp[-\mu(d_0 - d_m)], \quad (4)$$

$$D_s(d, r) = \sum_{r=0}^{r_m(\theta)} \sum_{\theta=0}^{2\pi} G f(x, y) RF(d, r) [SMR(d, r + \Delta r) - SMR(d, r)] \frac{\Delta\theta}{2\pi}. \quad (5)$$

Here

$$G_0 = [(SSD + d_m)/(SSD_0)]^2 \quad \text{and} \quad G_0 = [(SSD + d_m)/(SSD + d)]^2. \quad (6)$$

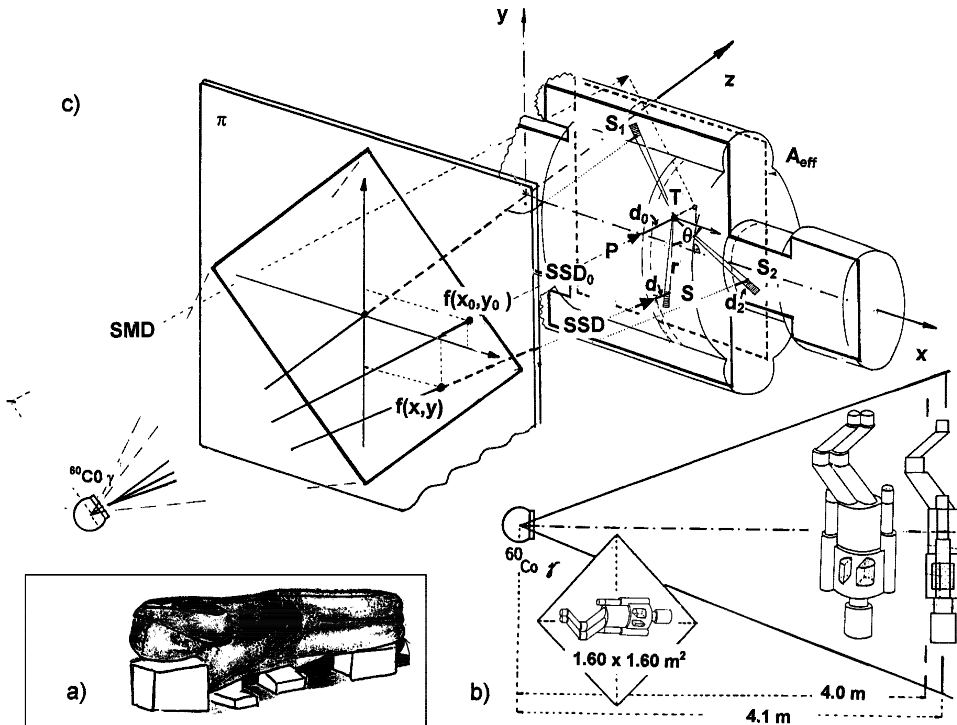


Fig. 2. (a) Experimental real anthropomorphic phantom filled with water (RAP). (b) Referential theoretical anthropomorphic phantom (RTAP). (c) Geometry of RTAP.

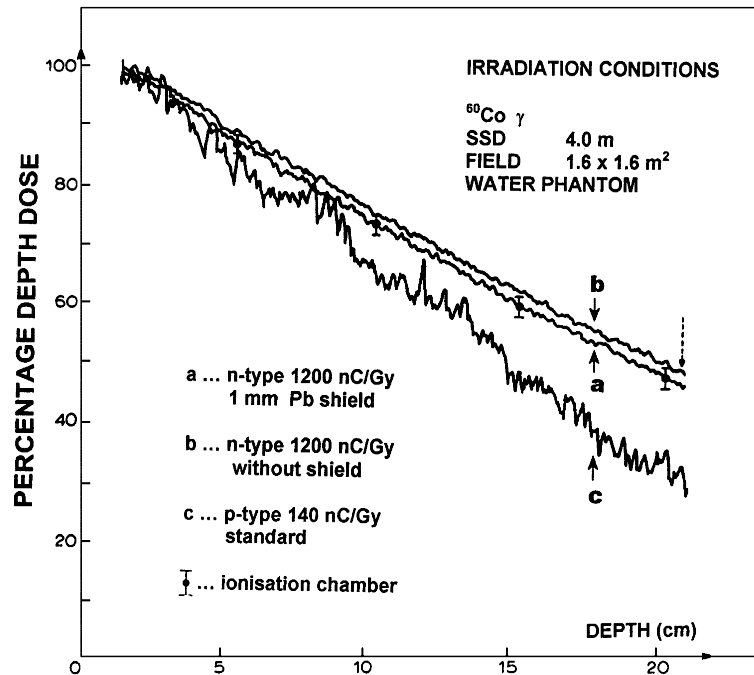


Fig. 3. Percentage depth dose in water as measured with various field detectors in low-dose-rate gamma field.

The explanation of the parameters in Eqs. (4), (5) and (6) is the following (see Fig. 2c):  $d_m$  is the buildup depth,  $f(x, y)$  is the off-axis (in air) dose distribution function which was measured in the plane in front of the phantom's entrance surface in buildup conditions at 156 points ( $1/8$  of  $160 \text{ cm} \times 160 \text{ cm}$  irradiation field at 400 cm from the source). The doses at other points (all together 1248) were available through symmetry and bilinear interpolation methods.  $SSD$  is the source-to-skin distance and  $SMD$  is the source-to-mid-plane distance,  $RF(d, r)$  are the experimentally-determined reduction-of-dose factors because of the lack of scatter in phantoms of finite thickness along a certain beam ray. These factors were obtained from the literature [21], applied separately for each location, using the methods of interpolation to phantoms of various thicknesses and fields.  $RF(d, r)$  amounts between 0.9 and 1.0.  $SMR(r, d)$  is scatter-to-maximum ratio [22], i.e., it is defined as the ratio of the scattered dose at a given point at depth  $d$  in phantom to the effective primary dose at the same point at the reference depth of maximum dose.

The principle of the calculation is as follows. The contributions of scattered radiation correspond to surface elements in the dose determination plane (coordinates  $r, \theta$ ), entering different phantom's parts at various local  $d$  and  $AP$ . The value  $r(\theta)$  (at a fixed  $\theta$ ) was increased step by step and  $r_{\max}(\theta)$  was determined during the

program execution when the scattering contributions came to the value that could be considered negligible (we defined in advance an acceptable error, e.g.,  $10^{-6}$ ). After that, the calculation chain came over to the next value of  $\theta$ . So we found the mean  $r$  as an average of  $r_{\max}$  over all  $\theta$ , and the equivalent effective square field  $A_{\text{eff}}$ . This  $A_{\text{eff}}$  field, as the *RF*-defining parameter, is directly related to  $r$ , the effective radius that is responsible for the scattering contributions. Analytically expressed *SMR* values [23] were used in the program.

The dose to the lungs was calculated under the assumption of an equivalent depth in the lung  $d'$  and a local field radius  $r'$ ,

$$d' = d - d_{\text{lg}}(1 - \rho), \quad r' = \rho r + n\Delta r. \quad (7)$$

Here,  $d_{\text{lg}}$  is the thickness of lung layer with low density  $\rho$  and  $n$  is an integer which reaches its maximum value (as  $r_{\max}$ ) at the moment of program execution when the calculated single scattering contribution of  $\theta$  direction has no more significant influence to the total scattering. The acceptable accuracy can be achieved with  $\Delta r = 1$  cm. If we designate the doses in the lung region in homogeneous and inhomogeneous phantom by  $D(d)$  and  $D(d')$ , respectively, the lung correction factor is

$$CF = \frac{D(d', r')}{D(d, r)}. \quad (8)$$

As pointed out above, the *MDF* values depend on the geometrical and physical conditions of the applied TBI technique. Aside from the primary dose, scattering reflects the shape, characteristic dimensions and mass arrangement in the environment at the dose-determination point. Therefore, each location (e.g., abdomen at  $AP/2$  depth) has its own value of *MDF* as a consequence of local patient's (phantom's) width, surrounding volume, curvature of the body and tissue density at that place. The calculated *MDF* values have reproduced those measured in the referential experimental real anthropomorphic phantom (RAP) within 2.1% for all considered dosimetric locations.

As a further step, a generalized simulation with a number of similar phantoms, where all linear dimensions were proportionally scaled (from 0.667 to 1.333 with respect to the referential one), made it possible to systematically investigate different RTAPs corresponding to patient's lengths 100-200 cm and masses 20-140 kg. As the result, the *MDFs* and *CFs* under TBI condition were obtained, suitable for mid-plane dose determination and for an application in corresponding clinical cases.

### 3. Calibration of a special *n*-type silicon field detector

We used  $^{60}\text{Co}$  Alcyon II (CGR-GE) irradiation-unit, RDM-1F (Scanditronix) electrometer, which was connected to RK 83-05 ionization chamber and  $2 \times 5$  semiconductor patient dose detectors with two DPD-5 (Scanditronix) dose monitors for



input-output dose readings during in-vivo dosimetry. The radiation field dosimetry was performed with the use of a specially constructed n-type silicon semiconductor detector with increased sensitivity (1200 nC/Gy, Scanditronix). The idea of the design, production and investigation of such a detector arised from an inadequate sensitivity of a commercial p-type Si detector when applied to TBI conditions, i.e., on extended source-to-skin distances. There, under extreme low dose-rate conditions (1 – 3 cGy/min), the signal was very weak. This effect resulted in an unacceptable oscillating behaviour of percentage depth dose curve with the commercial p-type detector (Fig. 3). Namely, the p-type Si detector has a stable relative sensitivity as a function of the dose rate only in standard irradiation conditions (fields up to 40 cm  $\times$  40 cm at SSDs up to 100 cm) [18]. To avoid the problem, it was suggested to produce a semiconductor detector of an increased sensitivity. The reason why the producer decided to make n-type Si detector is not known to the author. However, the detector showed excellent properties in very low dose rate  $^{60}\text{Co}$  gamma fields at extended distances (in TBI). We investigated the sensitivity of this special detector (see Fig. 4) in the range from extra low dose-rate cobalt TBI irradiation to the dose rates of standard radiotherapy which were by a factor 100 larger than under the TBI conditions.

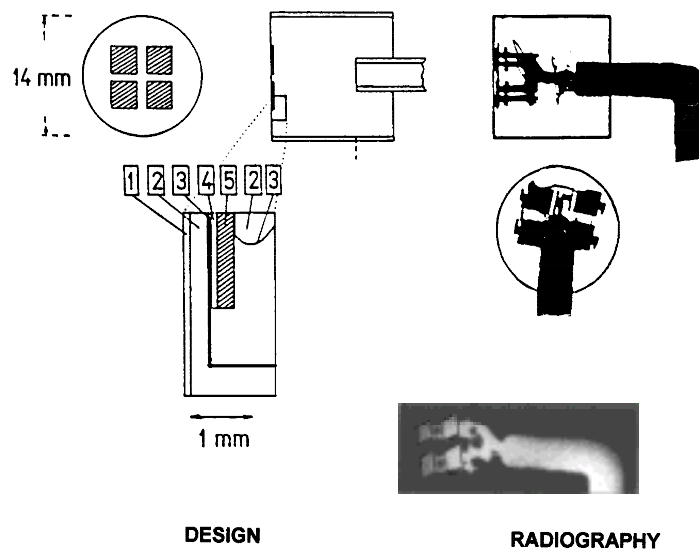


Fig. 4. Design, drawing and radiographic picture of the n-type Si field detector of an increased sensitivity (1200 nC/Gy): (1) water resistant paint, (2) detector body (epoxy resin  $1.2 \text{ g/cm}^3$ ), (3) thin ( $20 \mu\text{m}$ ) aluminium foil connected to a low-noise coaxial cable, (4) sensitive,  $50 \mu\text{m}$  thick ionisation volume, (5) Si crystal  $2.5 \text{ mm} \times 2.5 \text{ mm} \times 0.5 \text{ mm}$ .

Prior to the TBI procedure, a detailed radiation field analysis is required because of the non-standard conditions of the radiotherapy treatment. The geometry was

defined according to the protocol, so that at 400 cm from the source, the patient was lying on his side along a diagonal of the large 160 cm  $\times$  160 cm field. The measurements with the silicon detector were performed in a solid-water phantom (Gammex) at *SDDs* of 80, 100, 130, 160, 200, 267, 320 and 400 cm. The collimator openings generated the field dimensions 20 cm  $\times$  20 cm, 50 cm  $\times$  50 cm, 100 cm  $\times$  100 cm and 150 cm  $\times$  150 cm. As a high spatial resolution in this particular case is not needed, the relatively large sensitive area of the detector (diameter of 14 mm) was not a disadvantage and resulted in a decrease of the statistical noise and in a refinement of scale divisions on the electrometer (about 15 times as compared to the standard p-type detector or ionization chamber). In the 1 cm thick slab of solid water, a hole (that follows precisely the shape of the detector) was drilled, and detector placed in it, facing the source. Near the detector, an RK-83-05 ionization chamber was positioned in another hole of the front slab, and connected to the RDM-1F electrometer, to determine the absorbed dose by IAEA protocol [24]. Behind that, other 30 cm  $\times$  30 cm solid-water slabs were placed to form total thickness of 20 cm. Due to the reasons explained in the Introduction, the sidewalls of the detector were shielded with a cylinder of material with high *Z* (lead). It was found that 1 mm thick lead cylinder yielded the percentage depth-dose curves which agreed with the ionization chamber measurements (Fig. 3).

The calibration factor  $N_{\text{cal}}$  was obtained as the ratio of the absorbed dose  $D$  determined with the ionization chamber (corrected for temperature and pressure) and the Si detector reading  $M$ ,

$$N_{\text{cal}} = \frac{D}{M}. \quad (9)$$

We point out that relative sensitivity is often defined by reciprocal value, i.e.  $N_{\text{cal}}^{-1}$ .

The calibration factor  $N_{\text{cal}}$  of the investigated silicon detector was determined for a number of *SDDs* and field dimensions, defined at the front plane of the Si-detector position (as defined above). The possible number of measurements was limited by the maximal field dimension at a certain *SDD*. We represent the results in a form of the relative calibration factors, i.e., as  $N_{\text{cal}}$  normalized to the values at *SDD* = 400 cm and the field of 150 cm  $\times$  150 cm (Fig. 5). It follows that the first group of relative calibration factors for different field sizes (150, 100, 50 and 20 cm) which were determined at the TBI distance (*SDD* = 400 cm) in the dose rate range 1.59 – 2.00 cGy/minute, showed only the 1.9% deviation. In the second group (field sizes 100, 50, 20 cm at *SDD* = 300 cm) the deviation was 4.0%. At *SDD* = 267 cm and dose rate range 3.20 – 4.60 cGy/minute (field sizes 100, 50 and 20 cm), the deviation up to 7.3% was found. Other relative calibration factors of the corresponding fields at *SDDs* of 200 and 160 cm were found to be less suitable because of the maximal deviation of 10%. The use of the investigated detector at 130, 100 and at the standard distance of 80 cm (field size 20 cm  $\times$  20 cm) shows the worst behaviour with the 12.7% error. In the broad-beam  $^{60}\text{Co}$  gamma TBI, for the fields 100 cm  $\times$  100 cm, 130 cm  $\times$  130 cm and 150 cm  $\times$  150 cm, at *SDDs* of 267, 320 and 400 cm, the detector shows high stability (Fig. 6). The reproducibility error in all measurements was better than 1%.

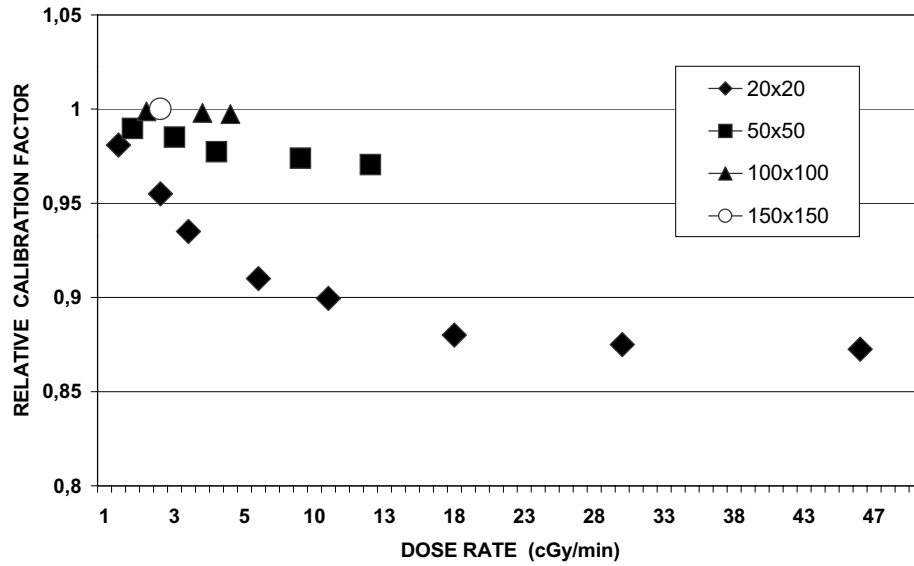


Fig. 5. Relative calibration factor, i.e.,  $N_{\text{cal}}$  normalised to  $N_{\text{cal}}$  values at  $SDD = 400$  cm and the field  $150 \text{ cm} \times 150 \text{ cm}$  as a function of the dose rate.

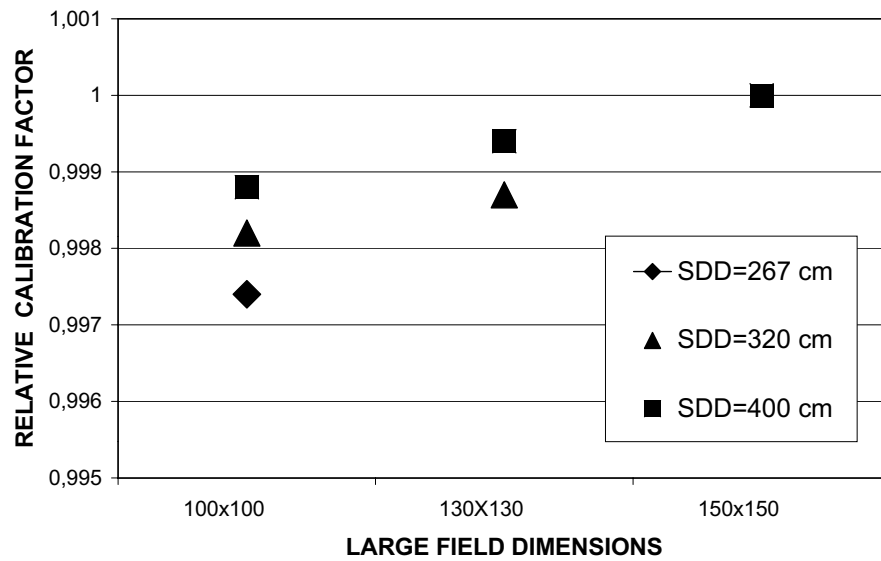


Fig. 6. Relative calibration factor normalised to the values at  $SDD = 400$  cm and field  $150 \text{ cm} \times 150 \text{ cm}$  as a function of large  $^{60}\text{Co}$   $\gamma$  field sizes.

#### 4. Conclusion

The procedure of TBI radiotherapy demands the radiation field dosimetry prior to the treatment with a special n-type silicon detector, which must be suitable to measure dosimetric data in the conditions different from the standard one. The obtained data have to be combined with (in advance) determined *MDF*'s of a real patient using the described software and results of in-vivo measurements during the treatment. Therefore, for the sake of completeness, the whole procedure of TBI irradiation was presented here. The investigated special n-type Si detector of an increased sensitivity (1200 nC/Gy) was found to be suitable for radiation field analysis in  $^{60}\text{Co}$  broad gamma beams under TBI conditions where the dose rate was relatively very low (1.59 – 2.00 cGy/min). In this region, the calibration factor showed a pronounced stability with a deviation of less than 2%, even in the case of extreme changes of field dimensions from 20 cm  $\times$  20 cm to 150 cm  $\times$  150 cm. The use of this detector in other cases, which are different from TBI, demands caution because of the rather large change in the calibration factor. This confirms the fact that various types of semiconductor detectors should be used, even for the same energy range, if the irradiation conditions (distance, field, and geometry) are drastically changed.

#### References

- [1] K. A. Johansson, W. F. Hanson and J. C. Horiot, *Radiother. Oncol.* **11** (1988) 201.
- [2] *ICRU Report 50*, ICRU, Washington (1993).
- [3] A. Dutreix, B. E. Bjarngard, A. Bridier, B. Mijnheer, J. E. Shaw and H. Svenson, *Physics for Clinical Radiotherapy*, booklet No. 3, ESTRO, IAEA, Leuven/Apeldoorn (1997).
- [4] B. J. Mijnheer, J. J. Battermann and A. Wambersie. *Radiother. Oncol.* **8** (1987) 237.
- [5] F. Sanchez-Doblado, U. Quast, R. Arrans, L. Errazquin, B. Sanchez-Nieto and J. A. Terron, in *Total Body Irradiation Prior to Bone Marrow Transplantation*, European Commission and European Group for Blood and Marrow Transplantation (EBMT), Sevilla (1995).
- [6] A. Dutreix and A. Bridier, *Path. Biol.* **27** (1979) 373.
- [7] A. Rizzoti, *Radiother. Oncol.* **5** (1985) 279.
- [8] P. Sverzelatti, G. Zonca, C. Stucchi, L. Gandola and F. Lombardi, in *Proc 2nd European Mevatron User's Conference*, Berlin, 14 – 16 January 1990, IZDAVAČ ?? (1990) 175.
- [9] J. A. Terron, F. Sanchez-Doblado, R. Arrans, B. Sanchez-Nieto and L. Errazquin, *Med. Dosim.* **19** (1994) 263.
- [10] M. Vrtar, *Adv. Radiol. Oncol.* **1** (1992) 323.
- [11] D. Fluhs, U. Quast and D. Szy, in U. Quast ed. *Dose to Lung, Proc. Seminar and Workshop on Physical Aspects of Total Body Irradiation*, Essen, 14 – 15 May 1990.
- [12] G. Marinello, A. M. Barie and J. P. Bourgeois, *J. Eur. Radiother.* **4** (1982) 174.
- [13] B. J. Mijnheer, R. K. Rice and L. M. Chin, in U. Quast ed., *Dose to Lung, Proc. Seminar and Workshop on Physical Aspects of Total Body Irradiation*, Essen, 14 – 15 May 1990 (PONAVALJA SE).

- [14] J. Van Dyk, T. Keane and W. D. Rider, *Int. J. Radiation. Oncology. Biol. Phys.* **8** (1982) 1363.
- [15] C. Jacob, G. Forcinal and J. Meuleman, *Nucl. Instr. Methods* **101** (1972) 51.
- [16] M. Osvay and K. Tarczy, *phys. stat. sol.* **27** (1975) 285.
- [17] L. Gager, A. E. Wright and P. Almond, *Med. Phys.* **4** (1977) 494.
- [18] G. Rikner, *Silicon Diodes as Detectors in Relative Dosimetry of Photon, Electron and Proton Radiation Fields*, Doctoral Thesis at Uppsala University (1983).
- [19] B. Labar, V. Bogdanić, D. Nemet, M. Mrsić, M. Vrtar, L. Grgić-Markulin, S. Kalenić, S. Vujasinović, V. Presečki, J. Jakić-Razumović and M. Marušić, *Bone Marrow Transplant.* **9** (1992) 343.
- [20] M. Vrtar and A. Purišić, *Radiotherapy and Oncology* **21** (1991) 157.
- [21] J. Van Dyk, P. Leung and J. R. Cunningham, *Int. J. Radiat. Oncol. Biol. Phys.* **6** (1980) 753.
- [22] M. Vrtar, *Doktorska disertacija, Sveučilište u Zagrebu* (1989).
- [23] J. R. Cunningham, *Phys. Med. Biol.* **17** (1972) 42.
- [24] M. Habič, A. Kmet and V. Smolej, *Phys. Med. Biol.* **19** (1974) 226.
- [25] *Absorbed Dose Determination in Photon and Electron Beams*, IAEA Technical Report Series No. 277, Vienna (1987).

DOZIMETRIJA OZRAČIVANJA CIJELOGA TIJELA GAMA SNOPOM  $^{60}\text{Co}$   
NISKE BRZINE DOZE

Postupak in-vivo dozimetrije, pri kojem se određuje doza u bolesnika tijekom samog ozračivanja, pomaže u procjeni razlike stvarne primljene doze i unaprijed propisane doze. To se postiže primjenom vanjskih mjerenja, tj. očitanjima ulaznih i izlaznih doza za pojedina područja tijela. U ovom se radu prikazuje metoda određivanja apsorbirane doze u bolesnika ozračenog velikim  $^{60}\text{Co}$ -gama poljem, kao i pri ozračivanju cijeloga tijela (ZCT), te analiza polja zračenja (prije stvarnog in-vivo postupka) na velikim udaljenostima od izvora, tj. pri niskim brzinama doze. Nov doprinos u tom području sastoji se u: (1) prilagodbi stvarnih anatomskih podataka određenog bolesnika (anterior-posterior debljine tijela u više točaka) teorijskom modelu antropomornog fantoma koji se sastoji iz niza eliptičkih cilindara i (2) uporabi specijalnog silicijskog detektora n-tipa s povećanom osjetljivošću kojim se analizira polje zračenja prije stvarnog in-vivo-ZCT postupka. Naime, standardni p-tip detektor, koji se komercijalno isporučuje i rutinski rabi za analizu polja zračenja na manjim udaljenostima i pri visokim brzinama doze, nije prikladan pri ZCT uvjetima gdje postoji niska brzina doze i slab signal. Zato se poklonila posebna pažnja ispitivanju ovisnosti kalibracijskog faktora specijalnog n-tip detektora o brzini doze u standardnim uvjetima ozračivanja i u uvjetima ozračivanja širokim poljima. Pokazalo se da je detektor prikladan za mjerenja u ZCT uvjetima. To se posebno potvrdilo u usporedbi ponašanja postotne dubinske doze pri mjerenjima sa spomenutim n-tipom i standardnim p-tipom detektora. Cjelokupni izloženi dozimetrijski model primijenjen je u praksi pri liječenju 350 bolesnika (uglavnom od leukemije) koji su bili ozračeni apsorbiranom dozom od 12.45 Gy u tri dana, u svrhu pripreme za transplantaciju koštane srži. Posebno niska brzina doze (između 1 i 3 cGy/min) uvjetovala je eliminaciju učestalosti iradijacijskog pneumonitisa, velike komplikacije u čitavom postupku liječenja (to ističu mnogi autori koji primjenjuju ozračivanja visokim brzinama doze).